

Levitation of quantum Hall critical states in a lattice model with spatially correlated disorder

Th. Koschny and L. Schweitzer

Physikalisch-Technische Bundesanstalt, Bundesallee 100, 38116 Braunschweig, Germany

(Dated: July 22, 2018)

The fate of the current carrying states of a quantum Hall system is considered in the situation when the disorder strength is increased and the transition from the quantum Hall liquid to the Hall insulator takes place. We investigate a two-dimensional lattice model with spatially correlated disorder potentials and calculate the density of states and the localization length either by using a recursive Green function method or by direct diagonalization in connection with the procedure of level statistics. From the knowledge of the energy and disorder dependence of the localization length and the density of states (DOS) of the corresponding Landau bands, the movement of the current carrying states in the disorder–energy and disorder–filling-factor plane can be traced by tuning the disorder strength.

We show results for all sub-bands, particularly the traces of the Chern and anti-Chern states as well as the peak positions of the DOS. For small disorder strength W we recover the well known weak levitation of the critical states, but we also reveal, for larger W , the strong levitation of these states across the Landau gaps without merging. We find the behavior to be similar for exponentially, Gaussian, and Lorentzian correlated disorder potentials. Our study resolves the discrepancies of previously published work in demonstrating the conflicting results to be only special cases of a general lattice model with spatially correlated disorder potentials.

To test whether the mixing between consecutive Landau bands is the origin of the observed floating, we truncate the Hilbert space of our model Hamiltonian and calculate the behavior of the current carrying states under these restricted conditions.

PACS numbers: 72.15.Rn, 71.30.+h

I. INTRODUCTION

A quantum Hall liquid system is believed to undergo a transition to a Hall insulator when the strength of the magnetic flux density B is turned to zero.^{1–5} This behavior was suggested by Khmelnitskii⁶ and Laughlin⁷ and explained in terms of a levitation scenario where, with decreasing B , the current carrying states float up in energy moving one by one across the Fermi level. Correspondingly, each time the Hall conductivity σ_{xy} drops by an amount e^2/h , until the last current carrying state gets depopulated and $\sigma_{xy} \rightarrow 0$. This notion provided the basic ingredient for the construction of a global phase diagram for the quantum Hall effect.⁸ In the quantum Hall liquid both the longitudinal conductivity σ_{xx} and resistivity ρ_{xx} get unmeasurable small in the limit temperature $T \rightarrow 0$, whereas the Hall insulator is characterized by a diverging resistivity $\rho_{xx} \rightarrow \infty$ while $\sigma_{xx} \rightarrow 0$.

However, some of the experimental results are not in accordance with the floating up picture. For example, direct transitions to the Hall insulator from higher ($\nu > 2$) quantum Hall plateaus have been reported^{9–11} as well as a saturation of the Landau level shift as $B \rightarrow 0$ for high quality p-GaAs samples.^{12,13} Recently, Yasin and co-workers¹⁴ have claimed that all the conflicting data published so far for different materials can be reconciled by a modified global phase diagram. They also find that the current carrying states continuously float up in energy as $B \rightarrow 0$, independent of the appearance of an apparent ‘metal’-insulator transition at $B = 0$.

On the theoretical side, the situation is still unclear. In particular, the microscopic origin of the floating remains obscure because the possible mechanisms put forward hitherto are only able to account for a very weak energetical shift, but not for the floating of the current carrying states across the Landau gap.^{15–18} Therefore, numerical investigations were

carried out in order to get some hint for the underlying physical process that causes the critical states to move upward in energy. Instead of studying the fate of the current carrying states when the magnetic field is decreased one can also look at the influence of an increasing disorder while B is fixed.^{19–28} In both cases, the Landau bands eventually start to overlap and the matrix elements connecting disorder broadened neighboring Landau bands become important.

The results of the numerical work for a disordered two-dimensional lattice model can be summarized as follows: There is a genuine floating of the critical states to higher energies.^{21,24,25,28–31} This floating is, however, not easy to observe in systems with uncorrelated random disorder potentials due to a peculiar annihilation mechanism inherent in the lattice model. In this model the Chern states, which correspond to the critical electronic states in each Landau band that are responsible for the integer quantized Hall conductivity, get neutralized by the so called anti-Chern states originating from the center of the tight-binding band. They move outwards in energy almost up to the band edges when the disorder strength is increased. Using spatially correlated random disorder potentials instead, it could be shown that the effect of the anti-Chern states is reduced so that the expected levitation scenario and the floating of current carrying states across the Landau gap is seen also in the lattice model.^{29,30} These results also imply that, contrary to other claims,^{23,26} the direct transitions to the Hall insulator occurring within the lattice model with uncorrelated disorder potentials can of course not be held responsible for the direct transitions seemingly observed in experiments.¹¹ Here, finite size effects and limited resolution due to finite temperatures are the most probable causes³² that account for the reported behavior.

The major aims of our work are fourfold: *i)* We have to check the universality of our previous results which were ob-

tained for a special model of exponentially correlated disorder potentials. Therefore, we study in the present work the influence of Gaussian and, to a lesser extent, Lorentzian like correlated disorder potentials in some detail. In particular, the results of the Gaussian disorder model will be useful when comparing with available analytical^{17,18} and recent numerical work where a 'universal quantitative relation' for the levitation of extended states has been proposed^{31,33}. Also, the correlated Gaussian model may likely become of greater importance to future analytical work on this subject because of the calculational advantage of Gaussian distributions compared to the exponential case.

ii) In our previous publication²⁹ the energetical shift of the current carrying states was obtained as a function of disorder strength and potential correlation length. However, the observed shift comprises the broadening effect of the total tight binding band and the floating up of the critical states in energy relative to the position of the density of states peak. To distinguish between these individual contributions and to address the question which of the possible definitions for the energetical shift^{19,21,31} are both reasonable and practicable, we have to calculate the density of states too. In addition we determine the levitation of the critical states as a function of filling factor that can be compared with experiments more easily.

iii) The general functional dependence of the levitation of the critical energy on disorder strength and magnetic field is unknown. Besides the conjectures independently suggested by Khmelnitskii⁶ and Laughlin⁷ there exists only some approximate analytical work for the weak levitation regime¹⁵⁻¹⁸. However, even within this limited range the various results partially contradict each other. Hence, for the advancement of this unsolved problem it seems adjuvant to numerically establish some empirical relations between disorder strength W , correlation length η , broadening of Landau levels Γ and the floating up in energy of the critical states. These relations, obtained for a well defined model, may then serve as a starting point for contriving much simpler models and later on as a benchmark for checking the outcome of subsequent analytical work.

iv) To provide a clue for a necessary microscopic explanation of the levitation scenario, we truncate the disordered lattice model and investigate how the floating up of critical states changes in the reduced model containing only one or two Landau bands. This approach simultaneously provides a new method for the scrutiny of the relevant matrix elements. This work is already in progress.

II. MODEL AND METHOD

The model consists of non-interacting electrons moving in the x - y -plane in the presence of disorder and a strong perpendicular magnetic field. This situation can be described by a Hamiltonian defined on the sites of a 2d lattice of size $M \times L$ with lattice constant a . Choosing the vector potential in the Landau gauge, $\mathbf{A} \equiv (0, -Bx, 0)$ with $(\nabla \times \mathbf{A})_z = B$, we

have

$$(H\psi)(x, y) = w(x, y)\psi(x, y) + V[\psi(x+a, y) + \psi(x-a, y) + \exp(-i2\pi\alpha_B x/a)\psi(x, y+a) + \exp(i2\pi\alpha_B x/a)\psi(x, y-a)], \quad (1)$$

where the magnetic field is chosen to be commensurate with the lattice size and $\alpha_B = a^2 e B / h$ denotes the strength of B expressed as the number of flux quanta h/e per plaquette a^2 . We mostly use $\alpha_B = 1/8$ in the present work and set the units of energy and length to $V = 1$ and $a = 1$, respectively. The on-site disorder potentials $w(x, y)$ are either uncorrelated or spatially correlated random numbers with probability density distributions as described in the next section.

The density of states $\rho(E, W, \eta)$ has been calculated by direct diagonalization of square systems of linear size $M = 64$ applying periodic boundary conditions in both directions. For the calculation of the localization length we utilize a recursive Green function method^{34,35} which allows to determine the transmission through very long ($L \sim 10^7$) quasi-one-dimensional systems of width M in the range $48 \leq M \leq 192$ from which the energetical position of the extended states can be extracted using a finite size scaling procedure.

The inverse localization length as a function of energy, disorder strength, and correlation length is defined as the exponential decay of the trace over the modulus of a sub-matrix of the one-electron Green function

$$\lambda_M^{-1}(E, W, \eta) = - \lim_{L \rightarrow \infty} \frac{1}{2L} \ln(\text{Tr} |G_{1L}^+|^2). \quad (2)$$

G_{1L}^+ is the $M \times M$ sub-matrix of the Green function $G(E)^\pm = (E - H \pm i\epsilon)^{-1}$ acting in the subspace of the columns 1, L on the lattice. For the calculation of $\lambda_M^{-1}(E, W, \eta)$ periodic boundary conditions are applied only in the y -direction (width of the system).

In the case of the projected disordered Harper model we used square systems of linear size $48 \leq M \leq 96$ and applied the method of level statistics to determine the energetical position of the current carrying states. This information is contained in the probability density distribution of the energy spacings of neighboring eigenvalues. Previously, this powerful method has been successfully applied to the study of critical properties at certain metal-insulator transitions.³⁶⁻⁴⁰ We have checked that the results calculated by this method agree with the ones obtained by the recursive Green function method. However, with comparable amount of numerical effort, the energetical resolution achieved is better in the Green function technique.

III. CORRELATED DISORDER MODEL

For the generation of the random disorder potential an algorithm is required which computes spatially correlated random numbers with a known correlation function and an arbitrary correlation length, continuously adjustable from zero (the uncorrelated case) to finite values. To be used efficiently in

conjunction with the recursive Green function method which operates on narrow but very long stripes, the random potential has to be computed “on the fly”, i.e., without keeping the whole random number field in memory. We generated a correlated random potential on the lattice \mathcal{G} by averaging over uncorrelated random numbers $\varepsilon(\mathbf{m})$ associated with each lattice point using a suitable weighting function f . The new correlated random numbers are defined as

$$\xi(\mathbf{m}) := \frac{1}{N} \sum_{\mathbf{m}' \in \mathcal{G}} f(\mathbf{m} - \mathbf{m}') \varepsilon(\mathbf{m}') \quad (3)$$

with $\mathbf{m} = (m_x, m_y) \in \mathcal{G}$. The disorder potential is $w(\mathbf{m}) = W \xi(\mathbf{m})$, where W is the disorder strength and the uncorrelated random numbers $\varepsilon(\mathbf{m})$ are uniformly distributed over $[-1, 1]$. The exact normalization factor $N = \sum_{\mathbf{m} \in \mathcal{G}} f(\mathbf{m})$ allows a comparison of different disorder models and correlation lengths via the homogeneous distribution function $p_{\xi(\mathbf{m})}(z)$ (see below) and the second moment of the random potential. For long-range correlations ($\eta > 1$), N approaches the continuum limit ($\pi\eta^2$ for Gaussian correlations), but deviates considerably for small η , e.g., $\eta \leq 0.3$.

It is expedient to choose f isotropic, $f(\mathbf{m}) = f(|\mathbf{m}|)$ and vanishing outside some finite circle $|\mathbf{m}| < R$. This cutoff R makes the generation of the ξ local as we only need to keep a window corresponding to an area $2R$ times the lattice width in memory. The $\xi(\mathbf{m})$ have a local distribution of realizations $z \in [-1, 1]$ that, with increasing η , transforms from a box shape into a Gaussian. The form of the distribution function can well be approximated by

$$p_{\xi(\mathbf{m})}(z) \approx \frac{N}{4f(0)} \left\{ \operatorname{erf} \left(\frac{f(0)N^{-1} - z}{\sqrt{\frac{2}{3}(g_2[f] - f(0)^2 N^{-2})}} \right) + \operatorname{erf} \left(z \mapsto -z \right) \right\} \quad (4)$$

with a second moment $\langle \xi(\mathbf{m})^2 \rangle_{\xi} = g_2[f]/3$ and $g_n[f] = N^{-n} \sum_{\mathbf{m} \in \mathcal{G}^2} f^n(\mathbf{m})$. The shape of this distribution depends on the extent of the weighting function f , hence on the correlation length, narrowing with longer correlation. This means we need a larger W for stronger correlation in order to get comparable effects of disorder in the Hamiltonian.

Choosing $f(\mathbf{m}) = \Theta(R - |\mathbf{m}|) \exp(-|\mathbf{m}|^2/\eta^2)$ with sufficiently large R , we obtain correlated random numbers with an approximately (due to the underlying lattice) Gaussian correlation function

$$K_f(\mathbf{m}, \mathbf{m}') = \gamma^2 \left(\left[\frac{d_x}{2} \right]_1 + \left[\frac{d_y}{2} \right]_1 \right) \exp \left(-\frac{|\mathbf{d}|^2}{2\eta^2} \right), \quad (5)$$

with $\mathbf{d} = \mathbf{m} - \mathbf{m}'$ and $[s]_1 \in [0, 1)$ denoting the fractional part of the real number s . The $\gamma(\eta)$ are 0.0077, 0.70, and 0.97 for $\eta = 0.3, 0.7$, and 1.0, respectively, approaching $\gamma = 1$ for $\eta \gtrsim 2$. For the $g_2[f]$ we get 1.0, 0.42, 0.17, and 0.04 for $\eta = 0.3, 0.7, 1.0$, and 2.0, respectively.

A Lorentzian like correlated random potential can be constructed by choosing $f(\mathbf{m}) = \Theta(R - |\mathbf{m}|) \eta^2/(\eta^2 + |\mathbf{m}|^2)$.

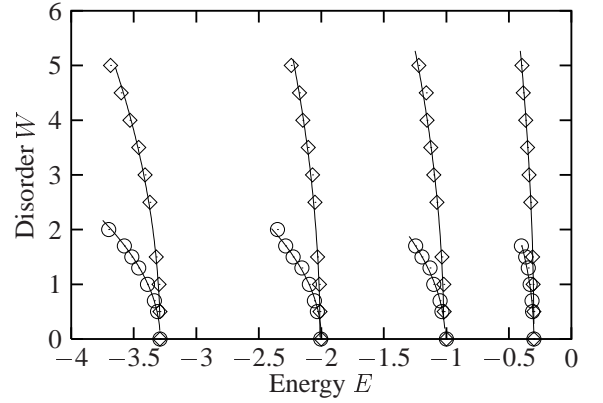


FIG. 1: The peak positions of the density of states $\rho(E, W, \eta)$ in the disorder (W) energy (E) plane. The DOS peaks move outwards (widening of the total TB band) with increasing disorder for a Gaussian correlation length $\eta = 0.3$ (\circ) and $\eta = 1.0$ (\diamond). The solid lines are quadratic fits $\delta E_n \propto -W^2$.

The corresponding correlation function is

$$K_f(\mathbf{m}, \mathbf{m}') \approx \frac{1}{\sqrt{\left(\frac{|\mathbf{m} - \mathbf{m}'|}{2\eta}\right)^2 + 1}} + o(|\mathbf{m} - \mathbf{m}'|).$$

In this case we have $g_2[f] = 2.9 \cdot 10^{-5}$ for $\eta = 1.0$.

IV. THE BEHAVIOR OF THE DENSITY OF STATES

Independent of the disorder model a non-zero disorder potential has two main effects on the density of states (DOS). First, the narrow Harper bands that replace the totally degenerated Landau levels of the continuum model on the lattice broaden nearly symmetrically. The total width of a sub-band consists of the intrinsic Harper broadening and the additional contribution due to the disorder potentials. For large correlation length the disorder induced sub-band broadening decreases with increasing Landau level index until the finite intrinsic width of the central Harper bands dominates. For small correlation length the disorder broadening is nearly independent of the Landau level index. The remaining difference in the observed sub-band broadening is associated with the varying intrinsic width of the unperturbed Harper bands. This usually leads to a slightly increasing width of the disorder broadened Harper bands with increasing proximity to the tight-binding (TB) band center. The shape of these sub-bands depends on the correlation length, becoming Gaussian for large η . Second, with increasing disorder strength the center position of the sub-bands move in energy towards the edges of the TB band. This effect is not small and stronger for the outer sub-bands.

The traces of the center positions of the disorder broadened Harper bands in the disorder-energy plane are plotted in Fig. 1. Because of the symmetry of the TB band, only the lower half is shown. The widening of the total TB band is proportional to the square of the disorder strength within the resolvable range.

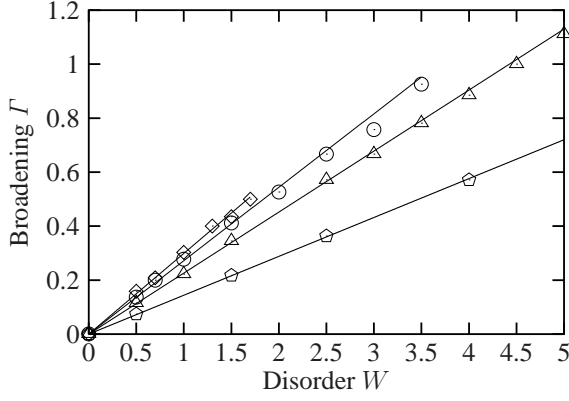


FIG. 2: The width Γ of the disorder broadened lowest Harper band vs. disorder strength W for different Gaussian correlation lengths $\eta = 0.3$ (\diamond), 0.7 (\circ), 1.0 (\triangle), and 2.0 (\square). The solid lines are linear fits $\Gamma \propto W$.

The solid lines in the picture are fits $W \propto \sqrt{-\delta E_n}$ for each sub-band n , where δE_n is the shift in energy of the respective DOS peak position due to the disorder W . We note that δE_n gets gradually smaller with increasing Landau band index n . In contrast, the disorder broadening of each individual Harper band is only linear in the disorder strength, $\Gamma \propto W$. This holds with good accuracy within the accessible range of disorders, independent of the correlation length as shown in Fig. 2. The broadening of the Harper bands is stronger for shorter correlation length of the disorder potential, however, taking the narrowing of the random potential distribution function with increasing correlation into account, we find stronger broadening for larger correlation length if the second moments of the random potential distribution functions are set equal.

The independence of the observed linearity from the correlation length enables us to define an *effective* disorder strength $W_{\text{eff}}(W, \eta)$ which causes the same bandwidth $\Gamma(W, \eta) = \Gamma(W_{\text{eff}})$ of the lowest Harper band independent of the disorder.

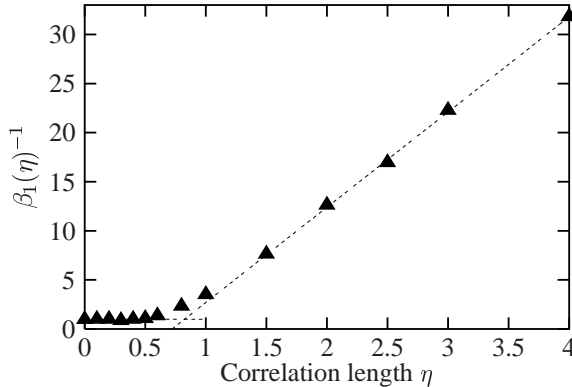


FIG. 3: The inverse of the pre-factor β_1 of the quadratic shift, $\delta E_1 = -\beta_1(\eta)\Gamma_1(W)^2$, of the DOS peak position of the first sub-band is shown as a function of the correlation length for Gaussian correlated disorder and fixed magnetic field $B = 1/8$. The dashed lines are partial linear fits.

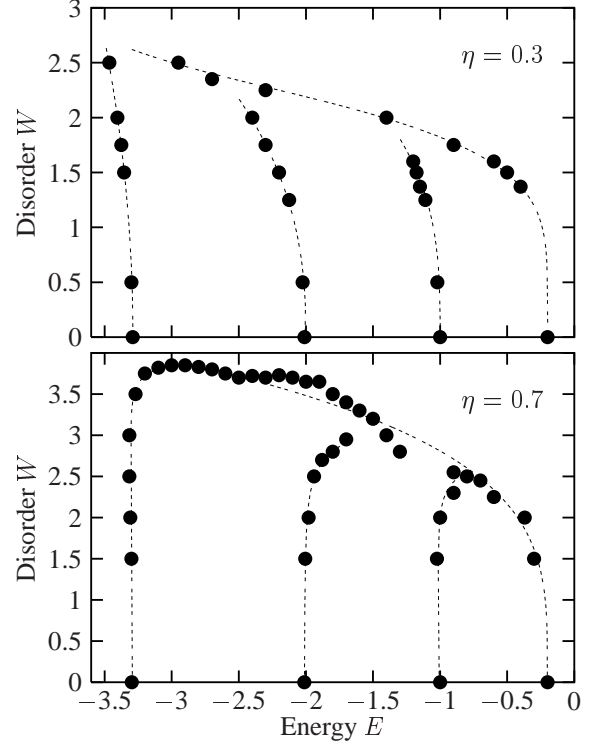


FIG. 4: The motion of the extended states with increasing disorder in the disorder-energy plane is shown for the lowest four Harper bands. The states starting at $E = -3.3$, $E = -2$, $E = -1$ are the Chern states, while the anti-Chern states start at $E \approx -0.2$. The Gaussian correlation lengths are $\eta = 0.3$ and 0.7 , respectively. The dashed lines are guides to the eye.

der model. This measure for the disorder strength allows the direct comparison between different correlations length and is also readily accessible from experimental data. For a given W_{eff} the spreading of the TB band decreases with increasing correlation length. For large correlation length ($\eta \gg 4$) the density of states can be described by the local distribution of the random potential folded with the unperturbed Harper band structure. For Lorentzian and exponential correlation, not shown here, we find qualitatively the same behavior of the DOS. Our results are also in agreement with investigations on continuum models.^{41,42}

Due to the linear broadening $\Gamma_1 \propto W$ of the lowest sub-band and the quadratic shift $\delta E_1 \propto -W^2$ of the peak position of its DOS as a function of disorder strength, the energetical shift is consequently quadratic in the sub-band's width, $\delta E_1 = -\beta_1(\eta) \Gamma_1(W)^2$. As shown in Fig. 3, the pre-factor $\beta_1(\eta)$ behaves for large correlation length like $\beta_1 \sim 1/\eta$, but saturates at a finite value for small correlation length.

V. THE BEHAVIOR OF THE CRITICAL STATES

The consideration of finite spatial correlations within the random disorder potentials resolves the discrepancy between the expectations of levitation of current carrying states within

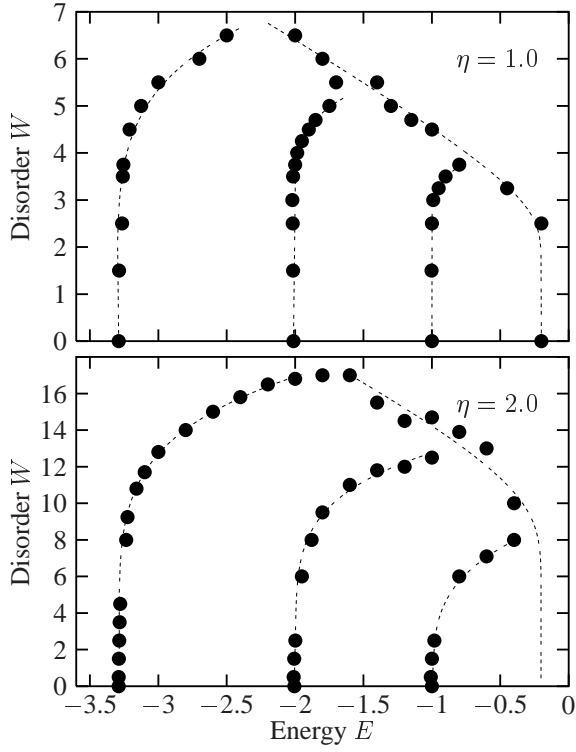


FIG. 5: The same as in Fig.4 with the exception that the correlation lengths of the Gaussian correlated disorder potentials are 1.0 and 2.0, respectively.

the continuum model^{6,7} and the downward moving anti-Chern states observed in lattice models with white noise disorder.^{19,20,22,23} We will show that both scenarios are only two special cases of the lattice model with correlated disorder that are associated with different spatial correlation lengths of the disorder potential.

In Figs. 4 and 5 the traces of the critical states for Gaussian correlated disorder are shown for several correlation lengths η in the disorder-energy plane. Again, the upper half of the tight-binding band is omitted as it is equal to the lower half mirrored at the line $E = 0$. For short correlation length $\eta = 0.3$, we find no levitation of the lower sub-bands which, in fact, move absolutely down in energy following the center position of the DOS peaks of the spreading TB band, though to a lesser extent. The anti-Chern states which reside near the band center for the Harper model without a disorder potential, rapidly move down in energy with increasing disorder strength, annihilating the Chern states from higher to lower Landau level index until eventually the last extended state vanishes near the band edge. For a slightly larger correlation length $\eta = 0.7$, the lower sub-bands stop moving downwards in energy and remain at their unperturbed energies up to a quite large disorder strength. The anti-Chern states still move quickly down with increasing W , but less rapidly than for smaller η . Only shortly before getting annihilated by the anti-Chern the extended states from the lower sub-bands start to move to higher energy. Now the last extended state is destroyed slightly above the energy of the lowest unperturbed

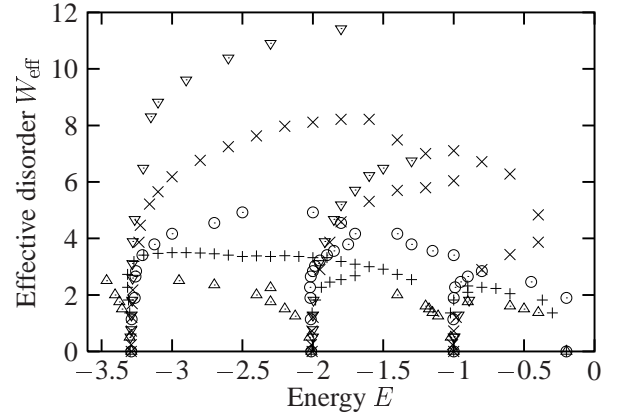


FIG. 6: The traces of the extended states (Chern and anti-Chern) vs. energy for different Gaussian correlation length, $\eta = 0.3$ (\triangle), 0.7 ($+$), 1.0 (\circ), 2.0 (\times), and 4.0 (∇) are compared using the effective disorder W_{eff} defined by an equal broadening of the lowest Harper band.

Harper band.

For longer correlation length (see Fig. 5) the extended states from the lower sub-bands strongly move up in energy while the anti-Chern states still move towards the band edges. The energy where the last extended state is destroyed when the lowest Chern and the anti-Chern states annihilate moves further towards the band center, passing the unperturbed 2nd Harper band energy for $\eta \approx 2$. If the correlation length is increased further the anti-Chern states remain too close to the band center to be resolved anymore, while the critical states of the lower sub-bands float up in energy clearly across the Landau gaps. Thus, for large correlation length, i.e., for smooth disorder potentials, we reach the levitation picture anticipated from the continuum model. From our data we see no indication for a merging of the critical states from the lower sub-bands in contrast to another report.⁴³

For sufficiently large correlation lengths and disorder strengths that produce equal widths of the lowest sub-band, the levitation of the 1st and 2nd critical states becomes slower with increasing η . This behavior is shown in Fig. 6. Also, the levitation gets stronger with increasing Landau level index. In contrast, the behavior is different for very small η and is probably dominated by lattice effects. Similar results have been obtained for other disorder models with exponentially²⁹ and Lorentzian like decaying correlation function.

In Fig. 7 the traces of the extended states' positions with respect to the filling factor are plotted. They clearly differ from the energy dependence (Figs. 4 and 5) since they contain the behavior of the extended states and the total DOS combined. As a function of the filling factor the observed levitation is even stronger because of the spreading of the tight-binding band and the additional rather small contribution originating from the accumulation of the density of states at a particular band that comes from sub-bands above (density floating^{19,20,24}). With respect to ν , the extended states from the lower band always levitate to higher fillings,³¹ even in the uncorrelated case. The prominent linear slope of the lower ex-

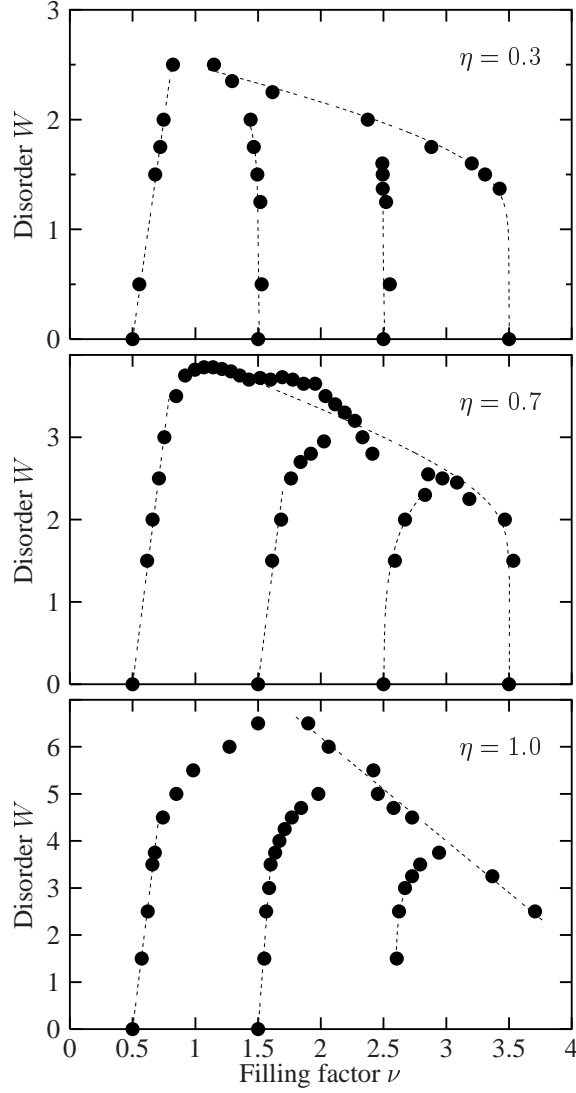


FIG. 7: The three figures show the behavior of the extended states in the disorder – filling factor plane for Gaussian correlation with $\eta = 0.3, 0.7$, and 1.0 . The dashed lines are guides to the eye.

tended states' traces for not too strong disorder is essentially an effect of the DOS behavior. The widening of the TB band $\propto W^2$ and the broadening of the Harper sub-bands $\propto W$ together with either the shift down in energy $\propto W^2$ ($\eta \leq 0.3$) or the absence of any movement ($\eta \geq 0.7$) leads for a qualitatively Gaussian like shape of the sub-bands to a prominent linear term $\propto W$ in the filling factor dependence for small W . This feature gets less pronounced for larger η .

For the disorder model with long-range Lorentzian like correlations, we find qualitatively the same behavior as for the Gaussian correlated random potential. The results are also compatible with those obtained previously for exponentially correlated disorder.²⁹ In Figs. 8 and 9 the traces of the extended states are shown vs. energy E and filling factor ν , respectively, for a correlation length $\eta = 1.0$. The levitation of the extended states from the lowest band across one and a

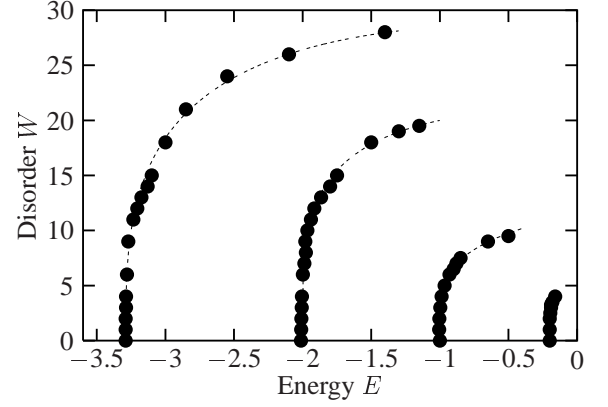


FIG. 8: The behavior of the current carrying states for a long-range Lorentzian like correlated background potential with correlation length $\eta = 1.0$ is shown in the disorder–energy plane. The downward movement of the anti-Chern cannot be resolved anymore. The dashed lines are guides to the eye.

half Landau gap in energy and even across two Landau gaps w.r.t. filling factor is clearly seen. Also, the second band's extended states can be traced nearly across one Landau gap in this case. The anti-Chern states from the TB band center are moving down too slowly with increasing disorder strength W to be resolved in this case.

VI. DISCUSSION OF THE RESULTS

The physical problem investigated here is governed by two fundamental scales, the energy scale $\hbar\omega_c/V$, which for the lattice model corresponds to $4\pi\alpha_B$, and the magnetic length $l_B/a = (2\pi\alpha_B)^{1/2}$, where $\alpha_B = p/q$ is the number of flux quanta per lattice plaquette a^2 . For strong magnetic flux densities $B = \alpha_B(\hbar/e)a^{-2}$, l_B gets smaller than the lattice constant a , a domain not considered in the present work. Here we

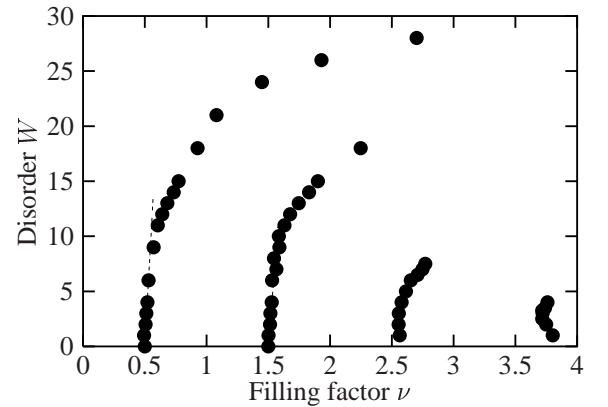


FIG. 9: The behavior of the current carrying states for a long-range Lorentzian like correlated background potential with correlation length $\eta = 1.0$ is shown in the disorder–filling factor plane. The dashed lines indicate the linear slope at small W .

have chosen $\alpha_B = 1/8$ which guarantees, in connection with spatially correlated disorder potentials and our presently available computer capacity, the ability to numerically resolve the entire ranges of energy and disorder values as shown above.

To discuss the influence of the correlation length of the disorder potentials one needs a practicable measure that allows the comparing of the various results. One choice is the second moment of the disorder potentials which is independent of B and can be viewed essentially as fixed for a given physical sample. A second possibility is the B -dependent disorder broadening of the sub-bands, $\Gamma \propto W$, which would be more advantageous in comparing with experiments. This method has been used in Fig. 6 where traces of the critical states have been plotted versus an effective disorder strength. However, for weak magnetic field and/or strong disorder this quantity may not easily be accessible.

In considering the observed energetical movement of the current carrying states E_c , one has to distinguish two contributions. One is related to the outward shift of the energetical position of the individual sub-bands of the DOS with increasing disorder strength, $\delta E_n \propto W^2$, which leads to the linear dependence on the filling factor ν . The second contribution is the absolute energetical shift, $\delta E_c = E_c - E_c(W = 0)$, of the critical states (Chern and anti-Chern states) across the Landau gaps. Both contributions depend on the correlation length of the disorder potentials and on the strength of the magnetic field. To compare with the energy shift proposed within the levitation scenario in the continuum limit,^{6,7} $\delta E \propto (n + 1/2)(\omega_c \tau)^{-2}$, the absolute energetical shift δE_c has to be considered. We find a qualitative agreement with this relation for larger correlation lengths η . For comparison with experiments, the calculated filling factor dependence of δE_c (see Figs. 7 and 9) seems to be better suited.

The levitation of the energy of the lowest current carrying states with respect to the sub-band peak of the density of states has recently been proposed to follow the relation³³

$$\frac{\delta E_{\text{eff}}}{\hbar \omega_c} \sim \frac{l_B}{\eta} \left(\frac{\Gamma}{\hbar \omega_c} \right)^2. \quad (6)$$

The definition of an effective shift δE_{eff} , given by the energy difference between position of the DOS peaks and the respective current carrying states^{21,31} is only practical as long as the DOS peaks can clearly be resolved which, however, gets increasingly problematic for small B and strong W . Therefore, it is clear, that this definition can, as a matter of principle, not be applied for the strong levitation across the Landau gaps seen in our investigation. In contrast, the resolution of the energetical position of the critical states can continuously be enhanced by applying larger system sizes. Our results also show that even in the weak levitation regime where the energetical shift of the critical states δE_{eff} is essentially due to the shift of the DOS peak δE_1 , the proposed linear relation $(\delta E_{\text{eff}})^{-1} \sim \eta$ only holds over a limited range of η . It strongly deviates for small η (see Fig. 3) where $\delta E_1 = -\beta_1(\eta)\Gamma^2$ saturates.

In the large disorder regime, where the strong levitation is dominated by the absolute energetical shift, even the relation $\delta E_c \sim W^2$ no longer holds. Instead, we clearly observe a

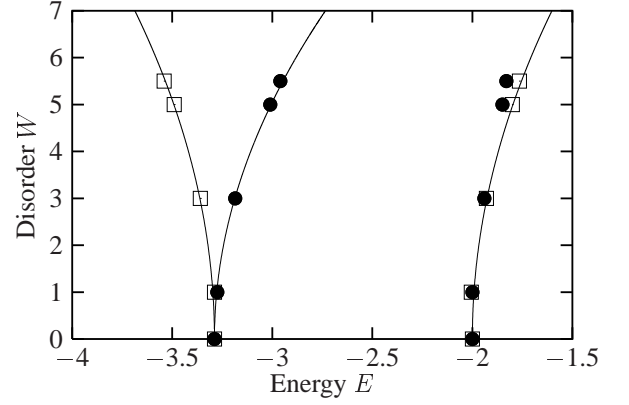


FIG. 10: The energetical positions of the DOS peaks (\square) and the positions of the critical states (\bullet) of the lowest two sub-bands for the projected disordered Harper model with correlation length $\eta = 1$ and magnetic field $B = 1/8$ are shown vs. energy E . The solid lines are the quadratic fits $\delta E \propto W^2$.

dependence with an exponent larger than 2. This behavior may change with decreasing B , but, due to the limited system size, it was not possible to resolve this problem yet. Finally, we did not see any merging of the levitating states, therefore true direct transitions are not possible. However, for smaller magnetic fields the critical states may get very close so that their resolution is not possible any more.

VII. PROJECTED DISORDERED HARPER MODEL

In order to get an idea of a possible mechanism that leads to the levitation of the critical states, we furthermore investigated a disordered Harper model projected onto the lowest few Landau levels. This was done by a projection of the highly non-diagonal spatial disorder potential within the base spanned by the unperturbed Harper eigenstates. Starting by using only the

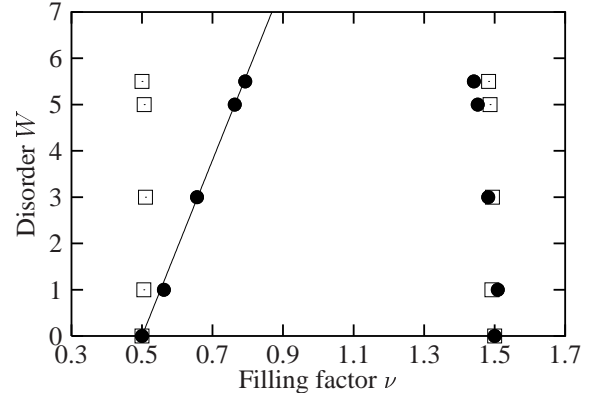


FIG. 11: For the projected disordered Harper model with correlation length $\eta = 1$ and magnetic field $B = 1/8$ the positions of the DOS peaks (\square) and the positions of the critical states (\bullet) of the lowest two sub-bands are shown vs. filling factor ν . The solid line is a linear fit $\delta \nu \propto W$.

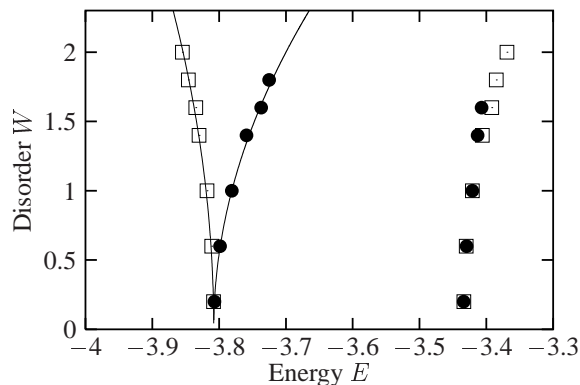


FIG. 12: For the projected disordered Harper model with correlation length $\eta = 1$ and magnetic field $B = 1/32$ the positions of the DOS peaks (\square) and the positions of the critical states (\bullet) of the lowest two sub-bands are shown vs. energy E . The solid lines are quadratic fits $\delta E \propto W^2$.

two lowest Harper bands, we could reproduce the widening of the total band as well as the levitation of the critical states of the lowest sub-band which is shown in Fig. 10 for a Gaussian correlation length $\eta = 1$. Since there are only two levels repelling each other, the center of the 2nd DOS peak moves to higher energies, in contrast to the full model. This widening leads to a shift of both sub-bands $\propto W^2$ as in the full model. The levitation of the lowest critical state is clearly visible while the extended states of the 2nd level are essentially following the DOS peak. Different from the full model, the levitation of the 1st level is with good accuracy $\propto W^2$ over the entire resolvable range. The levitation w.r.t. filling factor is again linear in W (Fig. 11). Further, we do not see any floating down of extended states for smaller correlation length as it has been observed for instance for Gaussian correlation with $\eta = 0.3$ in the full model (see Fig. 4).

Dropping the matrix elements describing the inter-band interaction of the disorder part in the Hamiltonian containing only two sub-bands, completely destroys the levitation as well as the widening of the total tight-binding band, while preserving the localization properties.

For a smaller magnetic field $B = 1/32$ the behavior of the disordered Harper model projected onto the lowest two Harper bands shown in Fig. 12 is qualitatively the same. However, the ratio of upward movement of the first sub-band's extended states and the downward movement of the corresponding DOS peak position changes with magnetic field. The shape of the traces remains purely quadratic in any case.

The addition of the third unperturbed Harper band to the projected model adds a qualitatively new behavior which is shown in Fig. 13. The DOS peak position of the second band remains nearly at the same energy, those of the first and third bands are moving outwards, while the extended states from the first and second bands move to higher energies and filling factors with increasing disorder strength. In the third band, the energy of the extended states essentially follows the DOS peak position. There is no indication for any absolute levitation of these extended states. This corresponds to the behavior of the

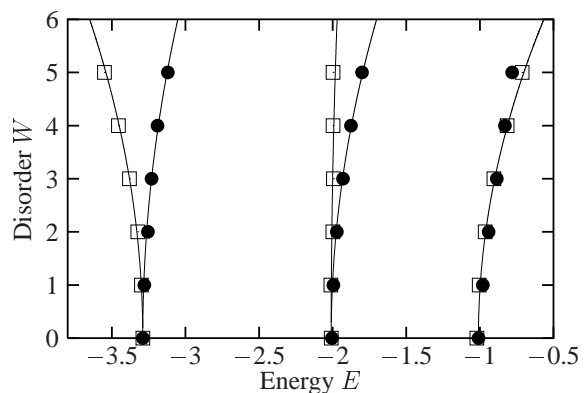


FIG. 13: For the projected disordered Harper model with correlation length $\eta = 1$ and magnetic field $B = 1/8$ the positions of the DOS peaks (\square) and the positions of the critical states (\bullet) of the lowest three sub-bands are shown vs. energy E . The solid lines are the quadratic fits $\delta E \propto W^2$.

second band in the two-band model shown above. The levitation of the lowest band's extended states is slowed down by the addition of a third band compared to the two-band model. Now it resembles closer the trace known from the full disordered Harper model (Fig. 4). We conclude, that in order to see levitation of a particular Harper band's extended states the existence of at least one adjacent band at higher energy is required.

VIII. CONCLUSIONS

The influence of spatially correlated disorder potentials on the levitation of current carrying states has been investigated for a quantum Hall system described by a two-dimensional lattice model. We considered what happens when the strength W of the disorder potentials is increased so that neighboring Landau bands start to overlap. Here, we showed our findings obtained mainly for spatially correlated disorder potentials which were generated with Gaussian correlations characterized by a correlation length η , but results for a Lorentzian like correlated disorder have also been presented. They both qualitatively agree with the previously obtained outcome for exponentially correlated disorder.^{28,29} Thus, the results obtained previously are not the consequence of the special exponentially correlated disorder model, but fit into a picture of a more general disordered lattice model which for long-range correlated disorder potentials agrees qualitatively with what is expected from the continuum model without a periodic background potential.

We numerically calculated the density of states $\rho(E, W, \eta)$ and studied the scaling of the localization length $\lambda_M(E, W, \eta)$ for various energies E , disorder strengths W , and system widths M from which the position of the critical states were extracted. Depending on the correlation length, we found three different cases. For small correlation length $\eta \lesssim 0.3$ no levitation of the Chern states, but their annihilation by downward moving anti-Chern states has been observed. For $\eta \gtrsim 2.0$ the Chern states float up in energy, at least across one

Landau gap. No effect of the anti-Chern states could be detected anymore for $\eta \geq 4$ where the anti-Chern remain close to the TB band center. In the latter case a levitation scenario as expected from the continuum model without a periodic potential has been observed in our lattice model. In the intermediate case $0.7 \lesssim \eta \lesssim 1.0$ both the levitation of the Chern as well as the outwards moving anti-Chern states can be noticed. As a function of the filling factor, the shift of the lower critical states is always positive, independent of the correlation length. One has to bear in mind that the levitation is always accompanied by the spreading of the tight-binding (TB) band, which is not negligible in particular for small η . We also have to mention that in contrast to a recent report⁴³ no merging of current carrying states was observed in our investigations. Therefore, no genuine direct transitions are possible within the present model. Of course, also the suggested annihilation mechanism of the current carrying states by anti-Chern states has to be discarded because this scenario is a special feature of the lattice model that cannot serve as an explanation for the experimental observations of a seemingly direct transition.

Besides these results that confirm and complement our previous findings for a model with exponentially distributed spatially correlated disorder potentials, we obtained the following new conclusions. *i)* The introduction of an effective disorder W_{eff} , which is defined by an equal broadening Γ of the sub-bands, allows a general discussion of the influence on the correlation length η . This is advantageous when comparing with other disorder models and experiment. The definition was possible only because of the observed linear broadening $\Gamma_1 \propto W$ for different Gaussian correlation lengths η . *ii)* The observed movement in energy of the current carrying states E_c consists of at least two contributions, the shift of the density of states peaks $\delta E_n \propto -W^2$, and the absolute energetical shift which for low disorders follows a relation $\delta E_c \propto W^2$. In the strong levitation regime at larger W , the absolute shift δE_c and therefore also the observed E_c move faster than W^2 . The peak of the lowest sub-band follows $\delta E_1 \propto -\beta_1(\eta)W^2$ with $\beta_1(\eta) \sim 1/\beta$ for η not too small, but saturates in the limit $\eta \rightarrow 0$. *iii)* The definition of an effective energetical shift of the current carrying states, i.e., $\delta E_{\text{eff}} \sim |E_1 - E_c|$ for the lowest sub-band, is practicable only for small disorder strength where the DOS peaks can be resolved. Therefore, it

does neither work in the medium and nor in the strong levitation regime across the Landau gap as observed in our work. Also, the proposed relation (Eq. 6) does not hold for small η where $(\beta(\eta))^{-1}$ is no longer linear in η . *iv)* Our study of the truncated disordered Harper model, which did not include the anti-Chern states, showed the levitation still to exist, provided the reduced model contains at least the coupling between the sub-band considered and the adjacent sub-band at higher energy. The spreading of the TB band as well as the levitation of the lowest critical states could already be detected in a model projected only onto the two lowest unperturbed Harper bands. Dropping the inter-sub-band interaction part of the correlated disorder potentials destroyed the levitation and the spreading of the TB band while preserving the localization properties. These results clearly show that the microscopic origin of the critical states' floating up in energy originates in the matrix elements of the disorder potentials constructed from eigenstates of consecutive Landau levels. In the case of the truncated lattice model the position of the critical states was extracted using the method of level statistics.

To summarize, we presented a comprehensive picture of the levitation of the current carrying states in the presence of spatially correlated disorder potentials. The behavior cannot be described by a simple general relation of the energetical shift as a function of magnetic field and disorder strength. However, empirical relations have been found which hold in certain ranges of the disorder and correlation length parameters. Further investigations, particularly at lower magnetic flux densities, are needed to clarify the complete functional dependences. Our results for the truncated disordered Harper model provide first clues for a microscopical understanding of the levitation of the current carrying states at the quantum Hall to insulator transition.

Acknowledgments

We acknowledge stimulating discussions with A. L. C. Pereira and P. A. Schulz. This work was supported in part by the Schwerpunktprogramm "Quantum-Hall-Systeme" of the German Science Foundation (DFG).

-
- ¹ H. W. Jiang, C. E. Johnson, K. L. Wang, and S. T. Hannahs, Phys. Rev. Lett. **71**, 1439 (1993).
 - ² A. A. Shashkin, G. V. Kravchenko, and V. T. Dolgoplov, JETP Lett. **58**, 220 (1993).
 - ³ T. Wang, K. P. Clark, G. F. Spencer, A. M. Mack, and W. P. Kirk, Phys. Rev. Lett. **72**, 709 (1994).
 - ⁴ R. J. F. Hughes, J. T. Nicholls, J. E. F. Frost, E. H. Linfield, M. Pepper, C. J. B. Ford, D. A. Ritchie, G. A. C. Jones, E. Kogan, and M. Kaveh, J. Phys. Condens. Matter **6**, 4763 (1994).
 - ⁵ I. Glozman, C. E. Johnson, and H. W. Jiang, Phys. Rev. Lett. **74**, 594 (1995).
 - ⁶ D. E. Khmelnitskii, Phys. Lett. **106A**, 182 (1984).
 - ⁷ R. B. Laughlin, Phys. Rev. Lett. **52**, 2304 (1984).
 - ⁸ S. Kivelson, D.-H. Lee, and S.-C. Zhang, Phys. Rev. B **46**, 2223 (1992).

- ⁹ D. Shahar, D. C. Tsui, and J. E. Cunningham, Phys. Rev. B **52**, R14372 (1995).
- ¹⁰ C. H. Lee, Y. H. Chang, Y. W. Suen, and H. H. Lin, Phys. Rev. B **58**, 10629 (1998).
- ¹¹ M. Hilke, D. Shahar, S. H. Song, D. C. Tsui, and Y. H. Xie, Phys. Rev. B **62**, 6940 (2000).
- ¹² S. C. Dultz, H. W. Jiang, and W. J. Schaff, Phys. Rev. B **58**, 7532 (1998).
- ¹³ Y. Hanein et al., Nature **400**, 735 (1999).
- ¹⁴ C. E. Yasin, M. Y. Simmons, N. E. Lumpkin, R. G. Clark, L. N. Pfeifer, and K. W. West, cond-mat/0204519 pp. 1–4 (2002).
- ¹⁵ T. V. Shahbazyan and M. E. Raikh, Phys. Rev. Lett. **75**, 304 (1995).
- ¹⁶ A. Gramada and M. E. Raikh, Phys. Rev. B **54**, 1928 (1996).

- ¹⁷ F. D. M. Haldane and K. Yang, Phys. Rev. Lett. **78**, 298 (1997).
- ¹⁸ M. M. Fogler, Phys. Rev. B **57**, 11947 (1998).
- ¹⁹ D. Z. Liu, X. C. Xie, and Q. Niu, Phys. Rev. Lett. **76**, 975 (1996).
- ²⁰ X. C. Xie, D. Z. Liu, B. Sundaram, and Q. Niu, Phys. Rev. B **54**, 4966 (1996).
- ²¹ K. Yang and R. N. Bhatt, Phys. Rev. Lett. **76**, 1316 (1996).
- ²² D. N. Sheng and Z. Y. Weng, Phys. Rev. Lett. **78**, 318 (1997).
- ²³ D. N. Sheng and Z. Y. Weng, Phys. Rev. Lett. **80**, 580 (1998).
- ²⁴ H. Potempa, A. Bäker, and L. Schweitzer, Physica B **256-258**, 591 (1998).
- ²⁵ K. Yang and R. N. Bhatt, Phys. Rev. B **59**, 8144 (1999).
- ²⁶ D. N. Sheng and Z. Y. Weng, Phys. Rev. B **62**, 15363 (2000).
- ²⁷ Y. Morita, K. Ishibashi, and Y. Hatsugai, Phys. Rev. B **61**, 15952 (2000).
- ²⁸ H. Potempa and L. Schweitzer, Physica B **298**, 52 (2001).
- ²⁹ T. Koschny, H. Potempa, and L. Schweitzer, Phys. Rev. Lett. **86**, 3863 (2001).
- ³⁰ T. Koschny and L. Schweitzer, Physica E **12**, 654 (2002).
- ³¹ A. L. C. Pereira and P. A. Schulz, Physica E **12**, 650 (2002).
- ³² B. Huckestein, Phys. Rev. Lett. **84**, 3141 (2000).
- ³³ A. L. C. Pereira and P. A. Schulz, Phys. Rev. B **66**, 155323 (2002).
- ³⁴ A. MacKinnon and B. Kramer, Phys. Rev. Lett. **47**, 1546 (1981).
- ³⁵ A. MacKinnon and B. Kramer, Z. Phys. B **53**, 1 (1983).
- ³⁶ B. I. Shklovskii, B. Shapiro, B. R. Sears, P. Lambrianides, and H. B. Shore, Phys. Rev. B **47**, 11487 (1993).
- ³⁷ I. K. Zharekeshev and B. Kramer, Phys. Rev. B **51**, 17239 (1995).
- ³⁸ M. Batsch, L. Schweitzer, I. Kh. Zharekeshev, and B. Kramer, Phys. Rev. Lett. **77**, 1552 (1996).
- ³⁹ J. W. Kantelhardt, A. Bunde, and L. Schweitzer, Phys. Rev. Lett. **81**, 4907 (1998).
- ⁴⁰ H. Potempa and L. Schweitzer, Phys. Rev. B **65**, 201105 (2002).
- ⁴¹ T. Ando, A. B. Fowler, and F. Stern, Rev. Mod. Phys. **54**, 437 (1982).
- ⁴² T. Ando, Journal of the Physical Society of Japan **53**, 3126 (1984).
- ⁴³ D. N. Sheng, Z. Y. Weng, and X. G. Wen, Phys. Rev. B **64**, 165317 (2001).